Magnetostatic excitations in quasiperiodic antiferromagnetic superlattices

S. S. Kang*
The Center for Materials for Information Technology, The University of Alabama, Tuscaloosa, Alabama 35487
(Received 1 May 2001; revised manuscript received 24 September 2001; published 3 January 2002)

The magnetostatic excitation in antiferromagnetic superlattices (antiferromagnetic/nonmagnetic layered structure) grown following the Fibonacci sequence has been studied. The dispersion relations of the magnetostatic spin wave spectra and the precession amplitudes of the total magnetization in each layer are numerically obtained. The eigenfrequency spectra are divided into two branches, ω^- and ω^+. For each branch, the distribution of eigenfrequency spectra exhibits triadic Cantor-set subband structures with self-similar features. The eigenfrequency spectra distribution strongly depends on the in-plane wave vector and the thickness of antiferromagnetic and nonmagnetic layers. For most of the eigenfrequencies, especially in the triadic regions, the profiles of precession amplitudes of total magnetization in the quasiperiodic system are critical and self-similar. For the eigenfrequencies near the edges of bands, the profiles of precession amplitudes of total magnetization are extended with a sine modulation. Besides the critical and extended states, a few states at the edges of the subbands are still quasilocalized. The corresponding profiles of precession amplitudes of total magnetization either decay or oscillate with exponential attenuation from the surface into the film.

DOI: 10.1103/PhysRevB.65.064401 PACS number(s): 75.50.Ee, 75.70.−i, 75.30.Ds, 76.50.+g

I. INTRODUCTION

The discovery of quasicrystals in 1984 aroused great interest,[1] both theoretically and experimentally, in quasiperiodic systems. For the electronic and phonon properties of the one-dimensional quasiperiodic system known as the Fibonacci chain or Fibonacci multilayers,[2–4] it has been found that both electronic and phonon spectra are Cantor-set structures[5] and the corresponding eigenstates may be localized, extended, or critical (neither localized nor extended). A quite complex fractal energy spectrum, which can be considered as their basic signature, is a common feature of these systems. Parallel with these theoretical developments in the field of quasiperiodic superlattices, experimental investigations have included diffraction, superconductivity, elasticity, and Raman scattering.[6–10] On the other hand, the collective excitations of the dipolar coupled ferromagnetic and antiferromagnetic superlattice have recently been discussed.[11–16] It has been found that both bulk and surface superlattice waves exist in the case where the saturation magnetization lies parallel to the layers in the superlattices. If the in-plane propagation wave vector of the spin wave is restricted to be perpendicular to the saturation magnetization, one finds that a bulk superlattice wave is composed of surface waves within each layer, and the amplitude of these surface waves varies sinusoidally throughout the layers of the superlattice. Similarly, a surface superlattice wave is composed of surface waves within each layer, but here the amplitude of the waves decreases exponentially as one penetrates into the superlattice. It exists only if the thickness of the antiferromagnetic layers is larger than that of the nonmagnetic layers. These features have been confirmed experimentally.[17–19] However, for the collective excitation in quasiperiodic superlattices, only little work has been done.[20,21] It is worthwhile to explore the magnetostatic excitation in the antiferromagnetic Fibonacci superlattices since these features might be detectable using microwave techniques, Brillouin scattering, or far-infrared experiments.[22–24]

In this paper, we have treated the problem of excitation in an antiferromagnetic superlattice with Voigt geometry: *The magnetostatic spin waves propagate along the surface of films and perpendicular to the applied field, which is also along the in-plane easy axis of films and less than the spin-flop field of the antiferromagnetic material to keep the antiparallel alignment of the spins of the two sublattices*. The recursion relations are deduced by the transfer matrix method. The eigenfrequency spectra and profiles of precession amplitude of total magnetization are obtained numerically. The triadic and self-similar eigenfrequency spectra strongly depend on the thickness of the antiferromagnetic and nonmagnetic layers. Three kinds of profiles of precession amplitude of total magnetization have been found: Critical states for most of the eigenfrequencies in the triadic subband; extended states near the edges of band; quasilocalized states (surface superlattice wave) at the edges of the subband. The results are discussed based on the invariant obtained analytically.

II. GENERAL THEORY

A Fibonacci superlattice is a simple one-dimensional quasiperiodic structure with two building blocks denoted by A and B. For the structure considered here, each of them is constructed by two layers with antiferromagnetic and nonmagnetic materials. The antiferromagnetic layers in A and B blocks have the same thickness, but the nonmagnetic layer has thickness d_1 in A block and d_2 in B block, respectively. Using these two blocks, a Fibonacci antiferromagnetic/nonmagnetic superlattice is formed according to the rule

$$S_{j+1}=\{S_j,S_{j-1}\};\ \ S_1=A;\ \ S_2=AB.$$

It is also invariant under the transformations $A\rightarrow AB$ and $B\rightarrow A$.[25] The Fibonacci generations are

$$S_1=[A],\ S_2=[AB],\ S_3=[ABA],\ S_4=[ABAAB],\ \text{ etc.}$$

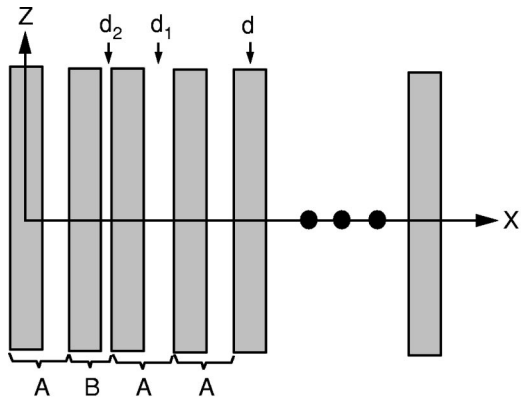

FIG. 1. The geometry of the Fibonacci superlattice. The thickness of the antiferromagnetic layer is d and the thickness of the nonmagnetic spacer is d_1 and d_2 in block A and B, respectively.

For our antiferromagnetic system, let the easy axis be the z direction, the wave vector be the y direction, and the quasiperiodicity be in the x direction (see Fig. 1). The sublattices are denoted by (I) and (II). For each cell, the total magnetization can be treated as: $m_i^T = m_i^I + m_i^{II}$ with $i = x,y$. In the magnetostatic limit,[15] Maxwell's equations can be expressed as

$$\nabla \cdot \mathbf{b} = 0, \quad \nabla \times \mathbf{h} = 0 \tag{1}$$

with the constitutive relation $\mathbf{b} = \vec{\mu}\mathbf{h}$, where $\vec{\mu}$ is the permeability tensor. If the fluctuation field has the time dependence of $e^{-i\omega t}$, where ω is the frequency, $\vec{\mu}$ has the form

$$\vec{\mu} = \begin{pmatrix} \mu_1 & i\mu_2 & 0 \\ -i\mu_2 & \mu_1 & 0 \\ 0 & 0 & 1 \end{pmatrix}. \tag{2}$$

Here

$$\mu_1 = 1 + \frac{4\pi\gamma^2 H_a M}{\omega_0^2 - (\omega + \gamma H_0)^2} + \frac{4\pi\gamma^2 H_a M}{\omega_0^2 - (\omega - \gamma H_0)^2},$$

$$\mu_2 = \frac{4\pi\gamma^2 H_a M}{\omega_0^2 - (\omega + \gamma H_0)^2} - \frac{4\pi\gamma^2 H_a M}{\omega_0^2 - (\omega - \gamma H_0)^2},$$

$$\omega_0 = \gamma\sqrt{2H_{\rm ex}H_a + H_a^2},$$

where H_a is the anisotropy field, $H_{\rm ex}$ is the exchange field, H_0 is the applied field, M is the saturation magnetization of one of the sublattices, and γ is the gyromagnetic ratio.

Equation (1) allows the introduction of a magnetic scalar potential $\mathbf{\Phi}$ defined by $\mathbf{h} = \nabla\mathbf{\Phi}$. From Eqs. (1) and (2), the scalar potential Φ obeys the equation of motion given by

$$\mu_1\left(\frac{\partial^2}{\partial x^2} + \frac{\partial^2}{\partial y^2}\right)\Phi + \frac{\partial^2}{\partial z^2}\Phi = 0. \tag{3}$$

The usual electromagnetic boundary conditions are that the tangential component of $\mathbf{h}$ and the normal component of $\mathbf{b}$ are continuous across any boundary along the x axis. So the boundary conditions can be writen in terms of the potential Φ as

$$\mu_1\frac{\partial\Phi^{\rm in}}{\partial x} - i\mu_2\frac{\partial\Phi^{\rm in}}{\partial y} = \frac{\partial\Phi^{\rm ex}}{\partial x}, \tag{4}$$

$$\Phi^{\rm in} = \Phi^{\rm ex}. \tag{5}$$

Here $\Phi^{\rm in}$ and $\Phi^{\rm ex}$ are the potential inside the antiferromagnetic and nonmagnetic layers, respectively.

Equation (3) is the equation of motion for Φ in both antiferromagnetic and nonmagnetic layers. Without loss of generality, we assume that only a plane wave e^{iky} propagates along the y direction with k as the in-plane wave vector. It is reasonable to write $\Phi = \phi(x)e^{i(ky-\omega t)}$ for both antiferromagnetic ($\Phi^{\rm in}$) and nonmagnetic ($\Phi^{\rm ex}$) layers. Equation (3) can be rewritten as

$$\left(\frac{d^2}{dx^2} - k^2\right)\phi(x) = 0. \tag{6}$$

The solution of Eq. (6) has the form $\phi_l(x) = A_l e^{k(x-x_l)} + B_l e^{-k(x-x_l)}$ in the antiferromagnetic layers, and $\phi_l(x) = C_l e^{k(x-x_l-d/2-d_i/2)} + D_l e^{-k(x-x_l-d/2-d_i/2)}$ $(i=1,2)$ in the nonmagnetic layers, where l denotes the block index and x_l is the intersection of midplanes of the lth antiferromagnetic layer with the x axis. If we eliminate C_l and D_l in the nonmagnetic layers using Eqs. (4) and (5), the coefficients of A_l, B_l and A_{l+1}, B_{l+1} of two adjacent antiferromagnetic layers are related by

$$\begin{pmatrix} A_{l+1} \\ B_{l+1} \end{pmatrix} = T(i)\begin{pmatrix} A_l \\ B_l \end{pmatrix}, \tag{7}$$

where $T(i)$ is a transfer matrix. For our system, $T(i)$ only has two different forms, $T(1)$ and $T(2)$, and their explicit forms are given as

$$T(i) = \begin{pmatrix} T_{11}(i) & T_{12}(i) \\ T_{21}(i) & T_{22}(i) \end{pmatrix} \quad (i=1,2), \tag{8}$$

where

$$T_{11}(i) = \{[(\mu_1+1)^2 - \mu_2^2]e^{kd_i} - [(\mu_1-1)^2 - \mu_2^2]e^{-kd_i}\}e^{kd}/(4\mu_1),$$

$$T_{12}(i) = (1+\mu_1-\mu_2)(1+\mu_2-\mu_1)(e^{kd_i} - e^{-kd_i})/(4\mu_1),$$

$$T_{21}(i) = (1+\mu_1+\mu_2)(1-\mu_2-\mu_1)(e^{-kd_i} - e^{kd_i})/(4\mu_1),$$

$$T_{22}(i) = \{[(\mu_1+1)^2 - \mu_2^2]e^{-kd_i} - [(\mu_1-1)^2 - \mu_2^2]e^{kd_i}\}e^{-kd}/(4\mu_1).$$

Both $T(1)$ and $T(2)$ are unimodular. As usual, we take $M_1 = T(1)$ and $M_2 = T(2)T(1)$, and have recursion relations $M_{j+1} = M_{j-1}M_j$, from which all M_j's can be obtained, where j is the Fibonacci generation number. Defining χ_j

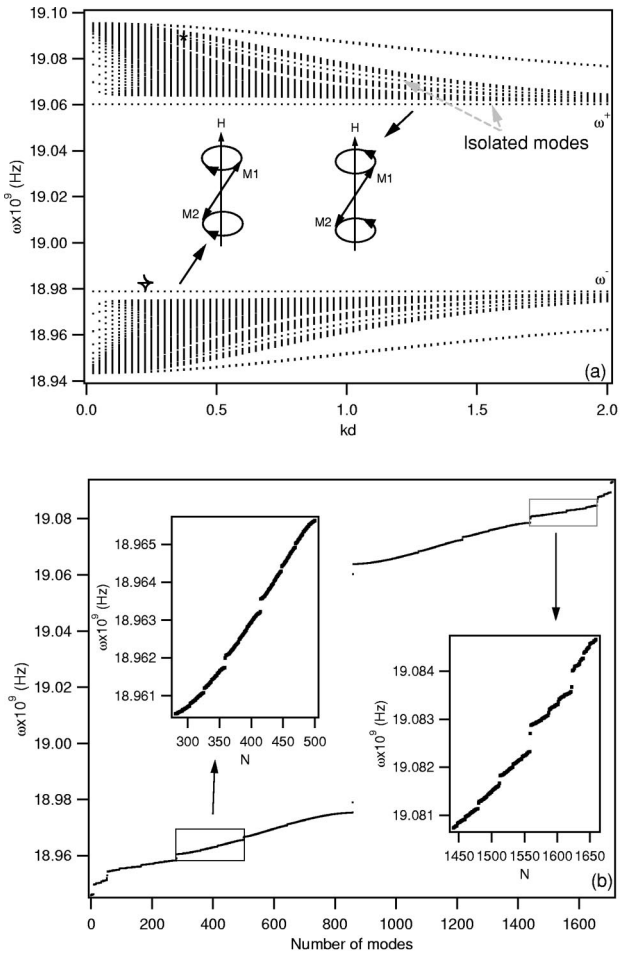

FIG. 2. (a) Dispersion relation of the eigenfrequency for the 12th order Fibonacci superlattice, here $d=4d_2, d_1=3d_2$. The * indicates the isolated mode is merged into subband modes. The insets are the profiles of precession of magnetization in two sublattices. (b) Eigenfrequency versus number of modes for 17th order Fibonacci superlattice with $kd=0.41, kd_1=0.375, kd_2=0.125$. Two enlarged local regions are shown in the insets.

$=\frac{1}{2}\mathrm{Tr}(M_j)$, one can find that the quantity $I=\chi_{j+1}^2+\chi_j^2+\chi_{j-1}^2-2\chi_{j+1}\chi_j\chi_{j-1}-1$ is invariant. For our system,

$$I=\frac{4\mu_1(\mu_1+\mu_2-1)(\mu_1-\mu_2-1)}{[4\mu_1+(\mu_1+\mu_2-1)(\mu_1-\mu_2-1)]^2}\times\sinh^2(kd)\sinh^2 k(d_1-d_2). \quad (9)$$

This analytic formula is different from those for electrons and phonons in Fibonacci chains.[26] This invariant has a wave vector dependence. It can be used to characterize the feature of the energy spectra as well as the properties of the states of Fibonacci superlattices.[26]

In the calculation of the frequency spectra of the Fibonacci antiferromagnetic superlattices, we use the free-boundary conditions. If N is the total number of antiferromagnetic layers in the jth order Fibonacci superlattice, by exploiting Eqs. (4) and (5) at the two surfaces, we can obtain the following two equations:

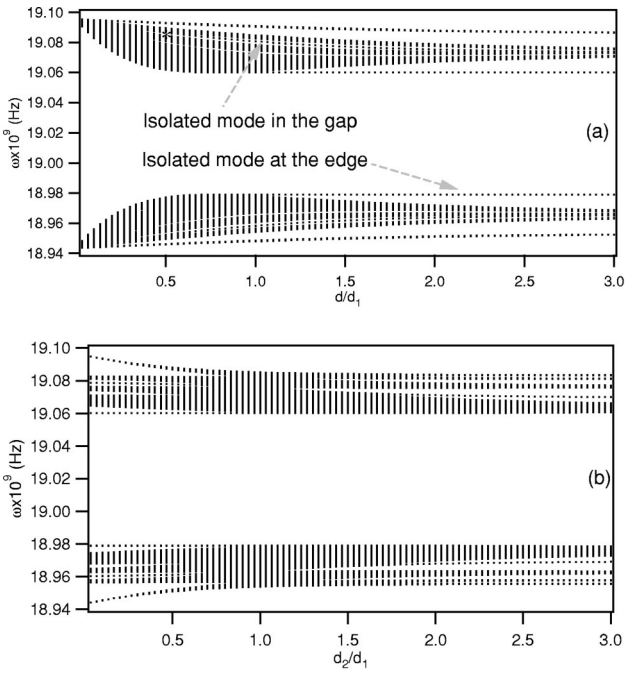

FIG. 3. The variation of eigenfrequency distribution with the thickness ratios (a) d/d_1 for $kd_1=0.6, kd_2=0.2$, (b) d_2/d_1 for $kd=0.8, kd_1=0.6$. The * indicates the isolated mode is merged into subband modes.

$$(\mu_1+\mu_2-1)A_1+(\mu_1-\mu_2-1)B_1e^{kd}=0, \quad (10)$$

$$(\mu_1+\mu_2+1)A_N+(\mu_1-\mu_2+1)B_Ne^{-kd}=0. \quad (11)$$

On the other hand, the global equation for the quasiperiodic structure can be writen as

$$\begin{pmatrix}A_N\\B_N\end{pmatrix}=M_j\begin{pmatrix}A_1\\B_1\end{pmatrix}. \quad (12)$$

The linear equations for A_1, B_1 and A_N, B_N, Eqs. (10), (11), and (12), have a nontrivial solution only if the determinant of the coefficient vanishes. By applying a numerical calculation, we can obtain the eigenfrequency spectra of the magnetostatic excitation. Here we select MnF_2 as the antiferromagnetic material. The physical parameters are $H_{ex}=550$ kOe, $H_a=7.87$ kOe, $M=600$ G, and $H_0=200$ Oe.[15]

III. RESULTS AND DISCUSSIONS

Figure 2(a) shows the dispersion relation of magnetostatic modes for the 12th order Fibonacci antiferromagnetic superlattice, where $d=4d_2$, $d_1=3d_2$, and d_2 are fixed. It is clear that the eigenfrequency spectra are divided into two branches, namely ω^- and ω^+, which are separated by a gap as in the periodic superlattices.[27] It can be seen that each branch consists of bandlike dense modes and *isolated* modes in the gaps. For larger kd, the modes are highly degenerate. For the intermediate value of kd, the subbands are most obvious, and hence the effect of quasiperiodicity is strongest. It is clear that the low frequency subband of the ω^- band is

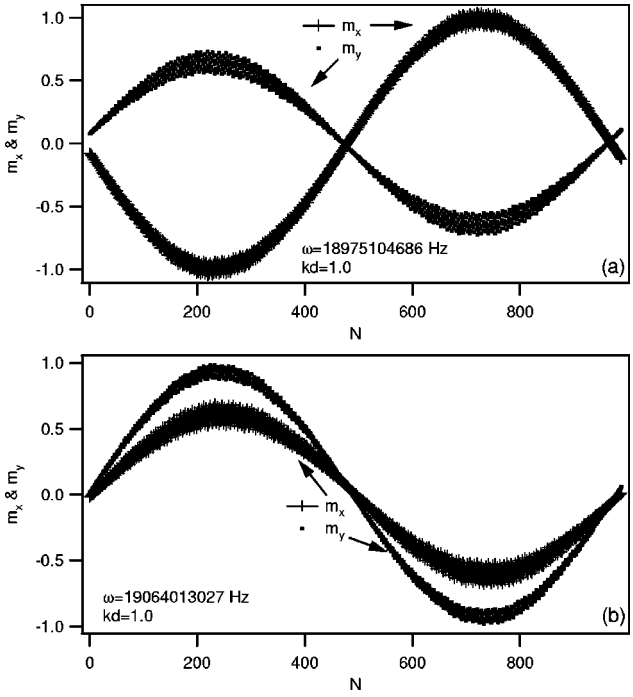

FIG. 4. The profiles of total magnetization (at midplane of each antiferromagnetic layer labeled with N) for eigenfrequencies in (a) ω^- band, (b) ω^+ band, here $d=4d_2, d_1=3d_2$.

wider than high frequency subband, but for the ω^+ band, the situation is reversed. This feature reflects the strength of quasiperiodicity, as can be illustrated by Eq. (9). The lower region of the ω^- band and the higher region of the ω^+ band have larger values of I, while the higher region of the ω^- band and the lower region of the ω^+ band have smaller values of I.

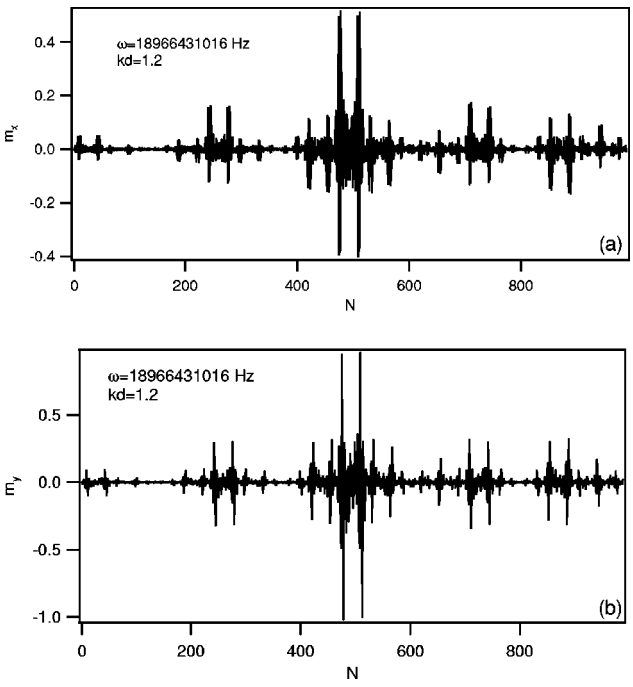

FIG. 5. The profiles of total magnetization (at midplane of each antiferromagnetic layer labeled with N) for the critical states: (a) m_x, (b) m_y, here $d=4d_2, d_1=3d_2$.

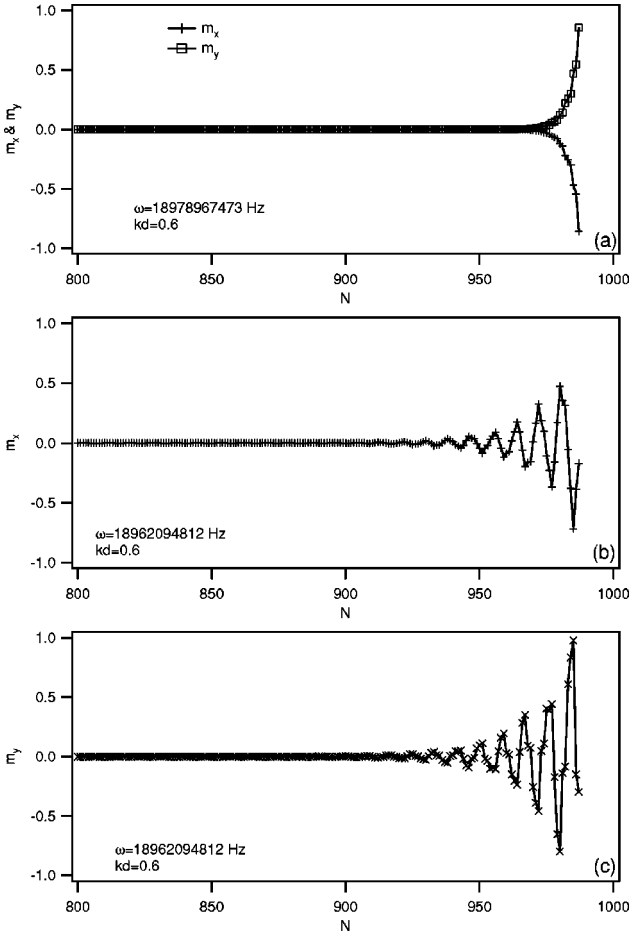

FIG. 6. The profiles of total magnetization (at midplane of each antiferromagnetic layer labeled with N) for two quasilocalized states corresponding to the eigenfrequencies (a) at the edge and (b), (c) in the gap, here $d=4d_2, d_1=3d_2$.

Figure 2(b) illustrates the eigenfrequency distribution with mode number. It is clear that the allowed frequency forms two branches of Cantor-set, which are singular continuous (the spectrum is between point and continuous).[28] For each branch, there are several bands. Each band has two gaps giving rise to three subbands, each one of them having two gaps and so on [see the inset of Fig. 2(b)]. This is the typical feature of a quasiperiodic system.[26]

The relative thicknesses of d, d_1, and d_2 have important effects on the eigenfrequency spectra. Figure 3(a) shows the eigenfrequency distribution with the thickness ratio d/d_1 for $kd_1=0.6$ and $kd_2=0.2$. It is clear that two branches of the eigenfrequency spectra consist of bandlike and *isolated* modes. For the *isolated* modes, two important features should be mentioned here. First, their appearance is closely related to the thickness of antiferromagnetic and nonmagnetic layers. When these parameters vary, some of the *isolated* modes can be merged into subband modes [see mark * in Fig. 3(a)]. Second, the *isolated* modes at the edges of two branches behave differently from *isolated* modes in gaps. When $d>d_1\&d_2$, the *isolated* modes at the edges of two

branches appear and their frequency almost does not change with the above parameters. But the frequency of *isolated* modes in gaps are obviously dependent on them.

Figure 3(b) shows the variation of eigenfrequency distribution with the thickness ratio d_2/d_1. When k, d, and d_1 are fixed, the eigenfrequency spectra are triadic branches as $d_2/d_1 \neq 1$. Notice that, for $d_2/d_1 \rightarrow 1$, two continuous bands are prominent, which stem from the fact that the structure becomes periodic (here $I \rightarrow 0$ as expected). However, the quasiperiodicity is more prominent for small or large values of d_2/d_1.

The quasiperiodicity of the frequency spectra must be reflected in the profiles of precession amplitude of total magnetization. According to Grünberg *et al.*,[12] the precession amplitude m_x and m_y of magnetization in the lth antiferromagnetic layer are given by

$$m_x = \frac{1}{4\pi}[(\mu_1+\mu_2-1)A_l e^{k(x-x_l)} + (\mu_2-\mu_1+1)B_l e^{-k(x-x_l)}], \tag{13}$$

$$m_y = \frac{1}{4\pi}[(\mu_1+\mu_2-1)A_l e^{k(x-x_l)} + (\mu_1-\mu_2-1)B_l e^{-k(x-x_l)}]. \tag{14}$$

We have calculated the total magnetization profiles for $j=15$ with different wave vectors. For the frequencies near the edges of two branches, due to the small constants of motion, the corresponding states are extended as illustrated in Fig. 4. It can be seen that the aperiodic amplitude is modulated by a sinelike wave. Thus the system behaves mainly like an ordinary periodic superlattice. For the ω^- band, the precession of total magnetization is elliptic and out-of-phase with the long axis along the x direction, while the precession is in-phase and elliptic with the long axis along the y direction for the ω^+ band. The corresponding precession of magnetization of the two sublattices is left (right) elliptic for the $\omega^-(\omega^+)$ band as illustrated in Fig. 2(a). As the frequency decreases (increases) from the edge of the $\omega^-(\omega^+)$ band, the modulation wavelength decreases approximately following the relation $\Lambda = 2D/n$ $(n=1,2,3,\ldots)$, where D is the total thickness of system.

As is the case in the electronic and phonon problem, we have found that most states are critical, especially in the obviously triadic subband. Figure 5 shows the profiles of the total magnetization. It is clear that the distribution of magnetization is neither sine extended nor an exponential decay, but it obeys a power law and is self-similar due to the quasiperiodicity.

As mentioned above, besides the extended and critical states, still a few states are quasilocalized. These states usually appear at the edges of the band or in the gaps of triadic subbands. Figure 6 shows two examples. For the quasilocalized states at the edge of bands, the profiles of precession exponentially decay from the surface [Fig. 6(a)]. This mode is unreciprocal and has its maximum amplitude at right surface for positive k and at the opposite surface for negative k.[29] The frequency is almost independent of the thickness of antiferromagnetic and nonmagnetic layers for $d > d_1 \& d_2$. However, for the quasilocalized states in the gaps, the profile of precession oscillates with an attenuating amplitude from the surface [Fig. 6(b)]. The frequency of the precession is sensitive to the thickness of antiferromagnetic and nonmagnetic layers as well as the in-plane wave vector.

In summary, we have investigated some interesting features of magnetostatic excitations in antiferromagnetic Fibonacci superlattices. It is found that the eigenfrequency spectra exhibit a triadic Cantor-set structure with nonuniform scaling and strongly depends on the thickness of antiferromagnetic and nonmagnetic layers. For the eigenfrequency in the obviously triadic region, the states are critical, whereas near the edges of bands, the states are extended like an ordinary periodic system. We also find a few states that are quasilocalized with the eigenfrequencies at the edges of bands or in the gaps of the subband. It might be possible to experimentally observe these predictions using Raman and Brillouin inelastic light scattering spectroscopy, ferromagnetic resonance, and far-infrared techniques.

ACKNOWLEDGMENTS

This work was supported by NSF MRSEC Grant No. DMR-9809423. The author would like to thank J. W. Harrell and J. A. Barnard for helpful comments.

*Corresponding author. FAX:+205-348-2346. Electronic address: skang@mint.ua.edu

[1] D. Shechtman, I. Blech, D. Gratias, and J.W. Cahn, Phys. Rev. Lett. **53**, 1951 (1984).

[2] P.M.C. de Oliveira, E.L. Albuquerque, and A.M. Mariz, Physica A **227**, 206 (1996).

[3] M. Quilichini and T. Janssen, Rev. Mod. Phys. **69**, 277 (1997).

[4] M.S. Vasconcelos and E.L. Albuquerque, Phys. Rev. B **57**, 2826 (1998).

[5] A Cantor-set is best characterized by describing its generation. Starting with a single line segment, the middle third is removed to leave behind two segments, each with length one-third of the original. From each of these segments, the middle third is again removed, and so on, *ad infinitum*. At every stage of the process, the result is self-similar to the previous stage, i.e., identical upon rescaling. This *triplet set* is not the only possible Cantor-set: any arbitrary cascaded removal of portions of the line segment may form the repetitive structure. See P. S. Addison, *Fractral and Chaos* (Institute of Physics, Bristol, 1997).

[6] R. Merlin, K. Bajema, R. Clarke, F-Y. Juang, and P.K. Bhattacharya, Phys. Rev. Lett. **55**, 1768 (1985).

[7] A. Hu, C. Tian, X.J. Li, Y.H. Wang, and D. Feng, Phys. Lett. A **119**, 313 (1986); R.W. Peng, A. Hu, S.S. Jiang, C.S. Zhang, and D. Feng, Phys. Rev. B **46**, 7816 (1992); J.W. Feng, G.J. Jin, A. Hu, S.S. Kang, S.S. Jiang, and D. Feng, *ibid.* **52**, 15 312 (1995).

[8] M.G. Karkut, J.M. Triscone, D. Ariosa, and O. Fischer, Phys. Rev. B **34**, 4390 (1986).

[9] H. Xia, X.K. Zhang, A. Hu, S.S. Jiang, R.W. Peng, W. Zhang, D.

Feng, G. Carlotti, D. Fioretto, G. Socino, and L. Verdini, Phys. Rev. B **47**, 3890 (1992).
[10] X.K. Zhang, H. Xia, G.X. Cheng, A. Hu, and D. Feng, Phys. Lett. A **136**, 312 (1989).
[11] R.E. Camley, T.S. Rahman, and D.L. Mills, Phys. Rev. B **27**, 261 (1983).
[12] P. Grünberg and K. Mika, Phys. Rev. B **27**, 2955 (1983).
[13] C. Mathieu, M. Bauer, B. Hillebrands, J. Fassbender, G. Güntherodt, R. Jungblut, J. Kohlhepp, and A. Reinders, J. Appl. Phys. **83**, 2863 (1999).
[14] E.L. Albuquerque, R.N. Costa Filho, and M.G. Cottam, J. Appl. Phys. **87**, 5398 (2000).
[15] B. Lüthi, D.L. Mills, and R.E. Camley, Phys. Rev. B **28**, 1475 (1983).
[16] S.P. Vernon, R.W. Sanders, and A.R. King, Phys. Rev. B **17**, 1460 (1978).
[17] P. Miltényi, M. Gruyters, G. Güntherodt, J. Nogués, and Ivan K. Schuller, Phys. Rev. B **59**, 3333 (1999).
[18] M. Grimsditch, M.R. Khan, A. Kueny, and I.K. Schuller, Phys. Rev. Lett. **51**, 498 (1983).
[19] G. Rupp, W. Wettling, W. Jantz, and R. Krishnan, Appl. Phys. A: Solids Surf. **37**, 73 (1985).
[20] S.J. Xiong, J. Phys. C **20**, L167 (1987).
[21] C.G. Bezerra and E.L. Albuquerque, Physica A **245**, 379 (1997); **255**, 285 (1998).
[22] J.R. Sandercock and W. Wettling, J. Appl. Phys. **50**, 7784 (1979); P. Grünberg and F. Metawe, Phys. Rev. Lett. **39**, 1561 (1977).
[23] J.P. Kotthaus and V. Jaccarino, Phys. Rev. Lett. **28**, 1649 (1972).
[24] M.G. Hildebrand, A. Slepkov, M. Reedyk, G. Amow, J.E. Greedan, and D.A. Crandles, Phys. Rev. B **59**, 6938 (1999).
[25] C.G. Bezerra, E.L. Albuquerque, A.M. Mariz, L.R. da Silva, and C. Tsallis, Physica A **294**, 415 (2001).
[26] M. Kohmoto, B. Sutherland, and C. Tang, Phys. Rev. B **35**, 1020 (1987).
[27] R.E. Camley and M.G. Cottam, Phys. Rev. B **35**, 189 (1987).
[28] R.E. Prange, D.R. Grempel, and S. Fishman, Phys. Rev. B **28**, 7370 (1983).
[29] M.G. Cottam and D.R. Tilly, *Introduction to Surface and Supperlattice Excitations* (Cambridge University Press, Cambridge, 1989).